RMETS
ROYAL METEOROLOGICAL SOCIETY

ENSO'S EFFECT ON ALASKA DURING OPPOSITE PHASES OF THE ARCTIC OSCILLATION

N. A. BOND[a],* and D. E. HARRISON[b]

[a] *JISAO, University of Washington, Seattle, Washington, 98195, USA*
[b] *NOAA/PMEL Seattle, Washington, 98115, USA*

ABSTRACT

The NCEP Reanalysis and station data are used to investigate how the winter weather of Alaska during El Niño/Southern Oscillation (ENSO) events has varied during different phases of the Arctic Oscillation (AO). Much greater 500-hPa geopotential height, 1000-hPa air temperature, and precipitation anomalies in association with ENSO tend to occur in the negative phase of the AO; these anomalies cannot be attributed to the AO on its own. Analysis of case-to-case variability indicates that the ENSO/AO composite results are robust. It is also shown that much of the variability of the 'Pacific pole' of the AO is associated with those winters with El Niño/AO- and La Niña/AO+ conditions, suggesting that this pole is much less robust than its counterpart in the North Atlantic. To the extent that winter mean state of the AO can be predicted, our results indicate that incorporation of the state of the AO would provide useful information for improving seasonal weather forecasts in the vicinity of Alaska. Copyright © 2006 Royal Meteorological Society.

KEY WORDS: ENSO; Arctic Oscillation; Alaska; winter weather

1. INTRODUCTION

The sources of interannual variability in the seasonal winter weather of Alaska and the Bering Sea are still being explored. Because of Alaska's proximity to the North Pacific, it is reasonable to suppose that it is significantly impacted by factors relating to fluctuations in the North Pacific atmospheric circulation. A dominant influence on the latter is El Niño/Southern Oscillation (ENSO) (Horel and Wallace, 1981, among many others), but statistical relationships between ENSO and the Alaskan weather have indicated rather modest signals. For example, the correlation coefficient between the Southern Oscillation Index (SOI) and mean winter temperature in Alaska is about -0.4, which is statistically significant but amounts to a modest average temperature anomaly of only $1-2\,°C$ (Papineau, 2001). The relationship between ENSO indices such as the SOI and winter sea ice cover in the Bering Sea is even weaker and less consistent (e.g. Niebauer *et al.*, 1999). On average, ENSO appears to modulate largely the intensity of the winter mean Aleutian low (Rogers, 1981), while the winter weather of Alaska and especially the Bering Sea is more sensitive to the position of the Aleutian low (Rogers, 1981; Rodionov *et al.*, 2005). Thus, it is useful to investigate other climatic factors than ENSO.

One factor that has been examined is the Pacific Decadal Oscillation (PDO) (Mantua *et al.*, 1997). Papineau (2001) found that El Niño winters in Alaska averaged about $1.4\,°C$ warmer than normal during the periods of 1925–1946 and 1977–1997, when the PDO tended to be positive; El Niño winters were about $0.6\,°C$ colder than normal from 1947 to 1976 when the PDO tended to be negative. These differences are comparable to the magnitude of the ENSO signal itself. Separating the effects of the PDO from those due to ENSO is

---

* Correspondence to: N. A. Bond, NOAA/PMEL, 7600 Sand Point Way NE, Seattle, WA 98115-6349, 1.206.526.6459, USA;
e-mail: nicholas.bond@noaa.gov

WILEY InterScience®
DISCOVER SOMETHING GREAT

problematic since the PDO on seasonal scales is correlated with ENSO. In fact, it has been suggested that the PDO reflects largely a low-pass filtered or rectified response to ENSO (Newman *et al.*, 2003). For the present study we focus on other potential influences on ENSO's effects.

The Arctic Oscillation (AO) (Thompson and Wallace, 1998) is another candidate source of seasonal variability for Alaskan winter weather. Previous work has examined the relationship between the AO and the Aleutian low (Overland *et al.*, 1999) and winter weather in the US and other regions of the Northern Hemisphere (Thompson and Wallace, 2001). The US weather anomalies associated with the AO also have been compared with those due to ENSO (Higgins *et al.*, 2002). Quadrelli and Wallace (2002) showed how the hemispheric expression of the AO (in their paper referred to as the Northern Hemisphere annular mode (NAM)) varies with the sense of ENSO.

Here we use the 1950–2005 observational record (the NCEP/NCAR Reanalysis and station data) to look further into the joint effect of ENSO and AO on winter (November–February) conditions in the vicinity of Alaska. The period 1950–2005 includes reasonably reliable information on the state of ENSO and the AO, and on the monthly mean atmospheric circulation. Winter here is taken to be from November through February because they represent the four coldest months for interior Alaska. We show that the interactions between ENSO and AO are complicated in that they do not simply reflect the superposition of separate effects. Our results are complementary to those of Quadrelli and Wallace (2002) in that they examined the modulation of the AO by ENSO while we examine how the effects of ENSO depend on the AO. Most of the work on AO/NAM has been on the hemispheric-scale or in the zonal mean sense; here we focus on Alaska because of the presence of large signals, as will be shown later. We examine the degree to which these signals are reliable for considering event-to-event variability and long-term trends. In an appendix we document how our ENSO/AO composites relate to fluctuations in the East Asian jet stream or EAJS (Yang *et al.*, 2002), the West Pacific (WP) Oscillation, and the PDO. The present work also bears on the issue of robustness of the Pacific pole of the AO (Deser, 2000; Wallace and Thompson, 2002).

2. SELECTION OF CASES FOR COMPOSITES

There is no universally accepted definition for the existence or strength of ENSO events. Widely used indices include the SOI that is based on sea-level pressure and the NINO3 and NINO3.4 measures of equatorial Pacific sea-surface temperatures (SSTs). Various multivariate indices have also been developed (e.g. the BEST index of Smith and Sardeshmukh, 2000; the BEI3 of Harrison and Larkin, 1998a). These multivariate indices can have the desirable property of better characterizing the combination of tropical atmosphere–ocean parameters that comprise the ENSO phenomenon.

Following the classification of Harrison and Larkin (1998a), an El Niño of moderate or greater intensity is identified to have occurred if the BEI3 exceeds 2.5 for a period of 3 months or longer. We consider the winters starting from the calendar year in which the BEI3 had reached the 2.5 threshold. By this definition, El Niño events occurred during the winters of 1957–1958, 1965–1966, 1969–1970, 1972–1973, 1976–1977, 1982–1983, 1987–1988, 1991–1992, and 1997–1998. These winters are widely considered as El Niño years in the literature referred. The winters of 1986–1987, 1994–1995, and 2002–2003 are also often considered to have featured El Niño. These three are the only other instances since 1950 in which the NINO3.4 anomaly was greater than 1 °C during October–February. The month of October is included for the NINO3.4 index because of the possible lag between tropical forcing and midlatitude response. The NINO3.4 index reflects conditions more in the central Pacific, and the BEI3 represents conditions more in the eastern Pacific. Present atmospheric numerical models tend to be particularly sensitive to SST in the NINO3.4 region.

With regard to La Niña, or cold ENSO events, we follow the procedure of Larkin and Harrison (2001). They identified cold events as those in which two out of three indices (Troup SOI, an SST index for the eastern equatorial Pacific, and NINO3.4) exceeded a threshold of $1\frac{1}{4}\sigma$ for three consecutive months. This criterion yields cold events in 1950–1951, 1954–1955, 1955–1956, 1964–1965, 1970–1971, 1973–1974, 1975–1976, 1988–1989, 1998–1999, and 1999–2000. The result of our procedure is a set of warm and cold events that are consistent with those previously identified and used by the climate community. Our results

are relatively insensitive to the exact make-up of the sets of events; the case-to-case variability is examined in Section 4 and in the Appendix.

We categorized the state of the AO during each ENSO event winter (November–February) using monthly and seasonal values available from NOAA's Climate Prediction Center (CPC) at http://www.cpc.ncep.noaa. gov/products/precip/CWlink/daily_ao_index/ao.index.html. The average values of AO during the ENSO events (November–February) defined above, and their values of NINO3.4, are summarized in Table I.

The atmospheric circulation for the various periods considered is summarized in the form of 500 hPa geopotential height, 1000 hPa air temperature, and precipitation rate anomaly maps based on the NCEP/NCAR Reanalysis data set as available at NOAA's Earth System Research Laboratory (formerly Climate Diagnostics Center) at http://www.cdc.noaa.gov/cgi-bin/PublicData/getpage.pl. This was also the source of the 200 hPa zonal wind data used to compute the EAJS index, and for monthly values of the WP index. As discussed by Kistler *et al.* (2001), the fields of tropospheric geopotential height and temperature are constrained by the observations in this reanalysis, and should agree with data from other reanalyses as carried out by the European Center for Medium-Range Weather Forecasting (ECMWF). Station data (monthly means) from six

Table I. Indices for the ENSO winters (NDJF)

Year	NINO3.4 (C)	AO	Z_{500} (m)	T_{AK} (C)
El Niño/AO−				
1957–1958	1.5	−1.1	−49.8	−16.5
1965–1966	1.5	−1.5	67.3	−20.5
1969–1970	0.8	−1.3	−73.3	−16.4
1976–1977	0.8	−2.0	−126.4	−12.1
1986–1987	1.2	−0.4	−74.7	−14.8
1987–1988	1.1	−0.5	−63.4	−16.2
1997–1998	2.6	−0.7	−73.0	−15.8
2002–2003	1.4	−0.8	−72.7	−11.4
Mean	1.4	−1.0	−58.2	−15.5
El Niño/AO+				
1972–1973	1.8	0.7	−1.6	−19.3
1982–1983	2.5	0.3	−104.0	−17.4
1991–1992	1.6	0.9	−50.0	−17.6
1994–1995	1.1	1.0	9.7	−17.8
Mean	1.8	0.7	−35.7	−18.0
La Niña/AO−				
1950–1951	−0.8	−0.7	65.6	−20.9
1954–1955	−0.9	−0.6	0.4	−18.7
1955–1956	−1.3	−1.2	118.1	−23.4
1964–1965	−0.8	−0.9	50.9	−22.7
1970–1971	−1.6	−0.3	96.3	−20.5
1973–1974	−1.8	−0.1	59.2	−21.7
Mean	−1.2	−0.6	65.1	−21.3
La Niña/AO+				
1975–1976	−1.5	0.9	−12.4	−22.5
1988–1989	−1.9	2.0	48.2	−18.8
1998–1999	−1.5	0.1	1.2	−19.1
1999–2000	−1.6	1.0	−11.9	−17.7
Mean	−1.6	1.0	6.3	−19.5

The values of NINO3.4 are in C; the AO index is normalized (by its monthly standard deviation). Z_{500} refers to the 500 hPa geopotential height anomaly for a rectangle extending from 45 to 55°N and 175 to 160°W; T_{AK} refers to the mean of air temperatures at Anchorage, Big Delta, Fairbanks, McGrath, Northway, and Tanana, Alaska.

locations, Anchorage, Big Delta, Fairbanks, McGrath, Northway, and Tanana, are used to describe surface temperatures over interior Alaska; station data from Cordova, Homer, King Salmon, Kodiak, Seward, and Yakutat are used to describe precipitation in southern Alaska. The source of the station data was NOAA's National Climatic Data Center (http://cdo.ncdc.noaa.gov/CDO/dataproduct).

3. COMPOSITE RESULTS

The anomalous atmospheric circulation over the central North Pacific and western portion of North America during ENSO depends on the phase of the AO, as can be seen in the maps for the average 500 hPa geopotential height anomaly (using a baseline period of 1968–1996) for the four different types of winters considered here (Figure 1(a–d)). During El Niño, both phases of the AO are associated with anomalously low 500 hPa heights extending from the Bering Sea southeastward into the North Pacific, but the center of the composite anomaly for AO− (Figure 1(a)) is deeper and located to the northwest of its counterpart for AO+ (Figure 1(b)). One of the consequences for Alaska is a much more prominent upper-airflow anomaly from the southeast during El Niño/AO−. Similarly, the 500 hPa height anomaly composites during La Niña indicate a positive center during AO− periods (Figure 1(c)), which is situated well northwest of its counterpart during AO+ periods (Figure 1(d)). The anomalous flow over Alaska during La Niña/AO− occurs strongly from the northwest and is almost a mirror to that occurring during El Niño/AO−, while for La Niña/AO+ this flow is weaker and from between the west and south.

The AO's impact on the effects of ENSO on atmospheric circulation is especially apparent through comparison maps of El Niño/La Niña differences. The average 500 hPa geopotential heights for the El Niño years minus those for the La Niña years for AO− and AO+ are shown in Figure 2(a) and (b), respectively. Note how the ENSO signal is much more prominent for Alaska and the Bering Sea during AO− than during
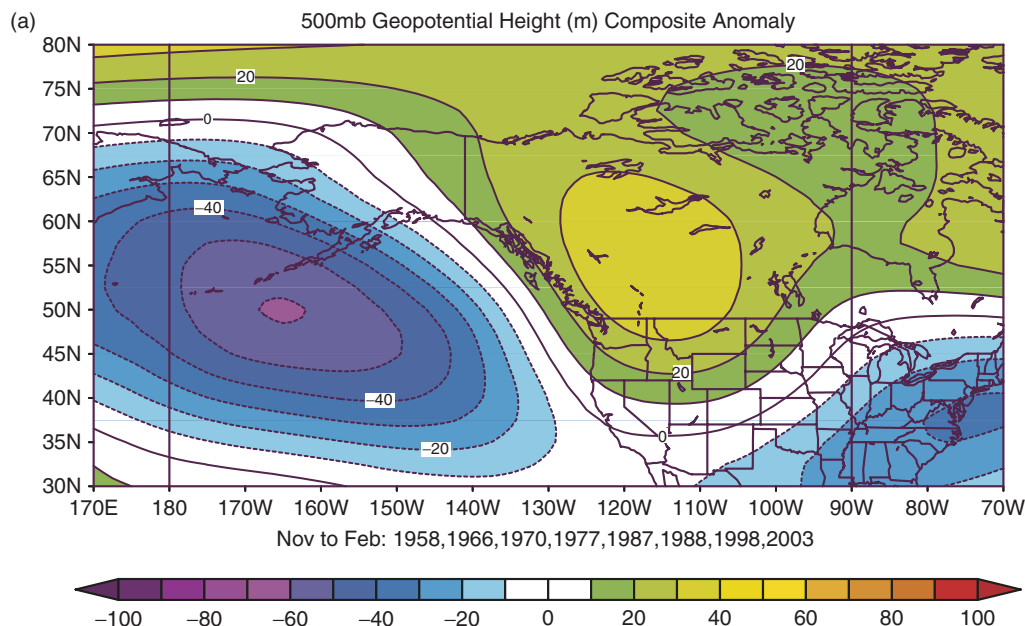

Figure 1. (a) Composite 500 hPa geopotential height anomalies (contour interval 10 m) during November through February for the El Niño/AO− winters of 1957–1958, 1965–1966, 1969–1970, 1976–1977, 1986–1987, 1987–1988, 1997–1998 and 2002–2003. Anomalies are relative to a baseline period of 1968–1996. (b) As in Figure 1(a), but for a composite of the El Niño/AO+ winters of 1972–1973, 1982–1983, 1991–1992, and 1994–1995. (c) As in Figure 1(a), but for a composite of the La Niña/AO− winters of 1950–1951, 1954–1955, 1955–1956, 1964–1965, 1970–1971, 1973–1974. (d) As in Figure 1(a), but for a composite of the La Niña/AO+ winters of 1975–1976, 1988–1989, 1998–1999, and 1999–2000
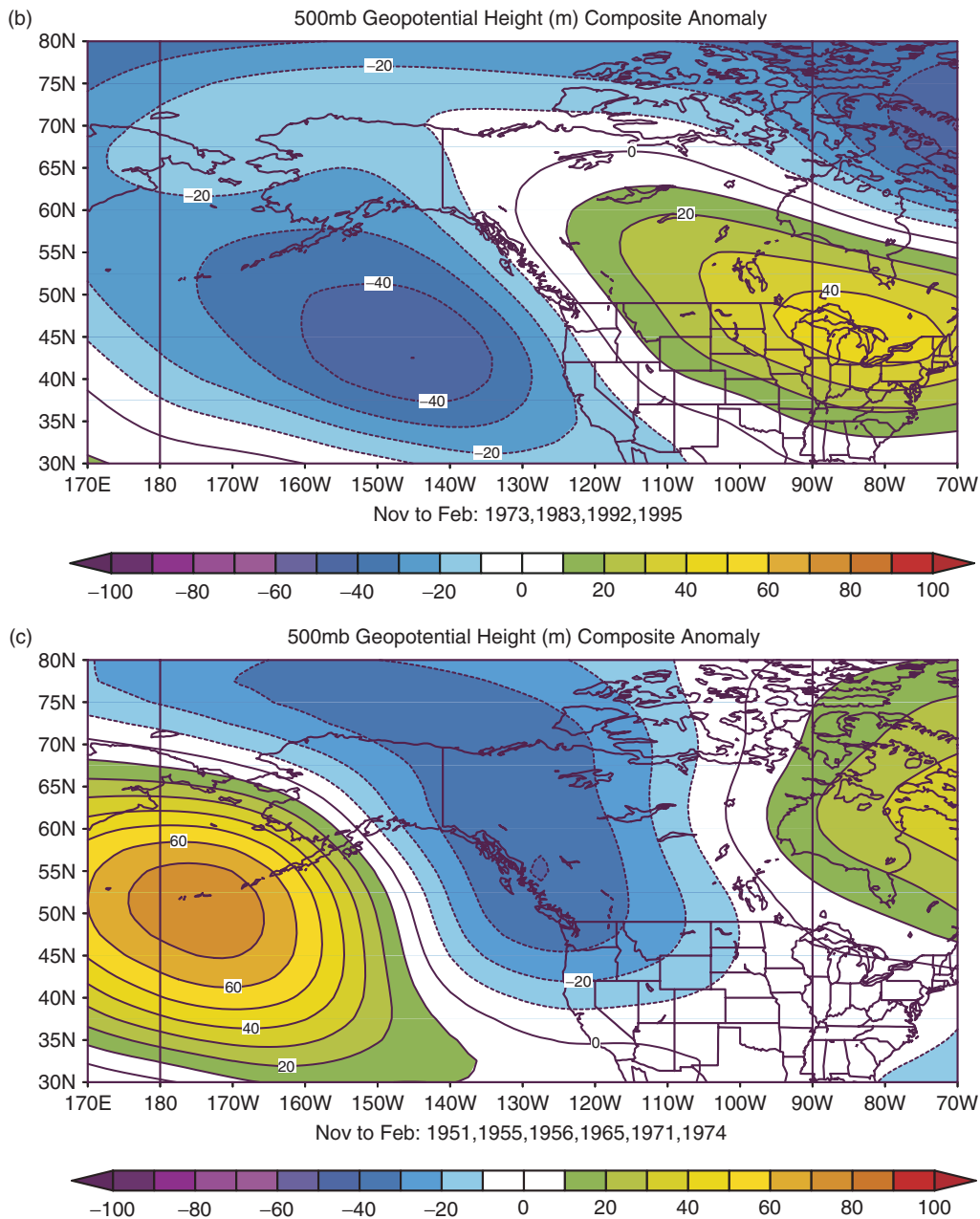
Figure 1. (*Continued*)

AO+ conditions. Of particular importance is the contrast in the position and intensity of the height anomaly centers, with implications for the 500 hPa flow anomalies in the two pairs of situations. Notably, the average meridional winds at 500 hPa over southern Alaska are 5–6 m s^{-1} from the south during the El Niño and 0–1 m s^{-1} from the north during the La Niña winters when the AO is negative (not shown); the effects of ENSO are more in the zonal component and weaker when the AO is positive.

The composite 500 hPa anomaly maps presented here regarding the interactions of ENSO and the AO are consistent with previous results. ENSO has been shown to be accompanied by systematic linkages or 'teleconnections' between the tropical Pacific and the global atmospheric circulation. In particular, negative
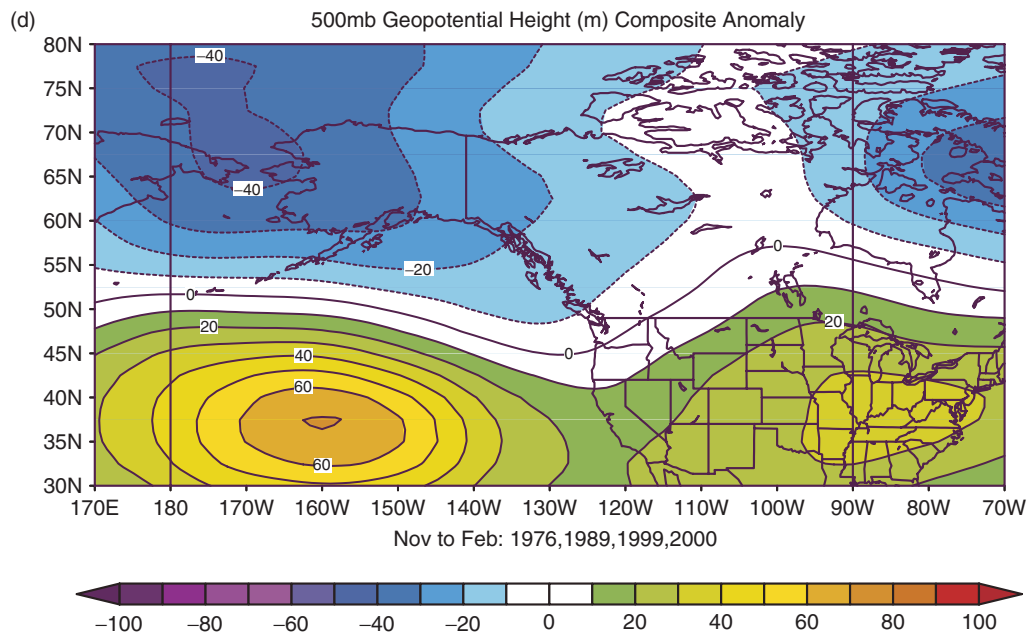
Figure 1. (*Continued*)

(positive) tropospheric height anomalies tend to occur south of the Aleutian Islands during El Niño (La Niña) winters (e.g. Horel and Wallace, 1981). As described above, height anomalies in this location have tended to be greater during negative phases of the AO. This can be attributed to the AO's effect on the character of the atmospheric circulation at middle to high latitudes. The negative phase of the AO is associated with an anomalously weak and asymmetric polar vortex and relatively high amplitude waves (e.g. Dole and Gordon, 1983) in the high-latitude circulation on timescales of weeks to months (Thompson *et al.*, 2002). This tendency for a less zonal flow during AO− in conjunction with a predisposition for height/pressure anomalies of a particular sense just east of the dateline with ENSO, can account for the differences illustrated in Figures 1 and 2.

As would be expected on the basis of 500 hPa anomaly maps in Figure 2(a) and (b), ENSO's impacts on low-level air temperature and precipitation near Alaska depend on the phase of the AO. This dependence is particularly striking in terms of the temperature over interior Alaska, where El Niño/La Niña temperature differences at 1000 hPa during AO− conditions (Figure 3(a)) are 2−3 times greater than those during AO+ conditions (Figure 3(b)). This result is also found in surface temperature records (data from a composite of six stations are presented in the following section; their locations are indicated in Figure 3(b)). Comparison of precipitation rates from the NCEP Reanalysis indicates much bigger impacts due to ENSO in southern Alaska for the AO− (Figure 4(a)) than for the AO+ (Figure 4(b)) winters. The different precipitation rates in southern Alaska from the Reanalysis shown in Figure 4(a) and (b) are supported by actual precipitation measurements. For example, the records from six southern Alaska stations (Cordova, Homer, King Salmon, Kodiak, Seward, and Yakutat; locations shown in Figure 4(b)) indicate a combined average El Niño/La Niña precipitation ratio of 1.88 in AO− conditions as compared with an average El Niño/La Niña precipitation ratio of 1.12 in AO+ conditions. For all six of these stations, both El Niño winters have been wetter on average during AO− than during AO+ conditions, and La Niña winters have been drier on average during AO− than during AO+ conditions.

In consideration of the AO's influence on the response to ENSO, it is necessary to account for the effects of the AO by itself. While the effects of the various modes of climate variability cannot be strictly separated on the basis of historical records, regression analysis represents a straightforward procedure for estimating the linear contribution of the AO to the differences shown in Figures 2 and 3. As indicated in Table I,
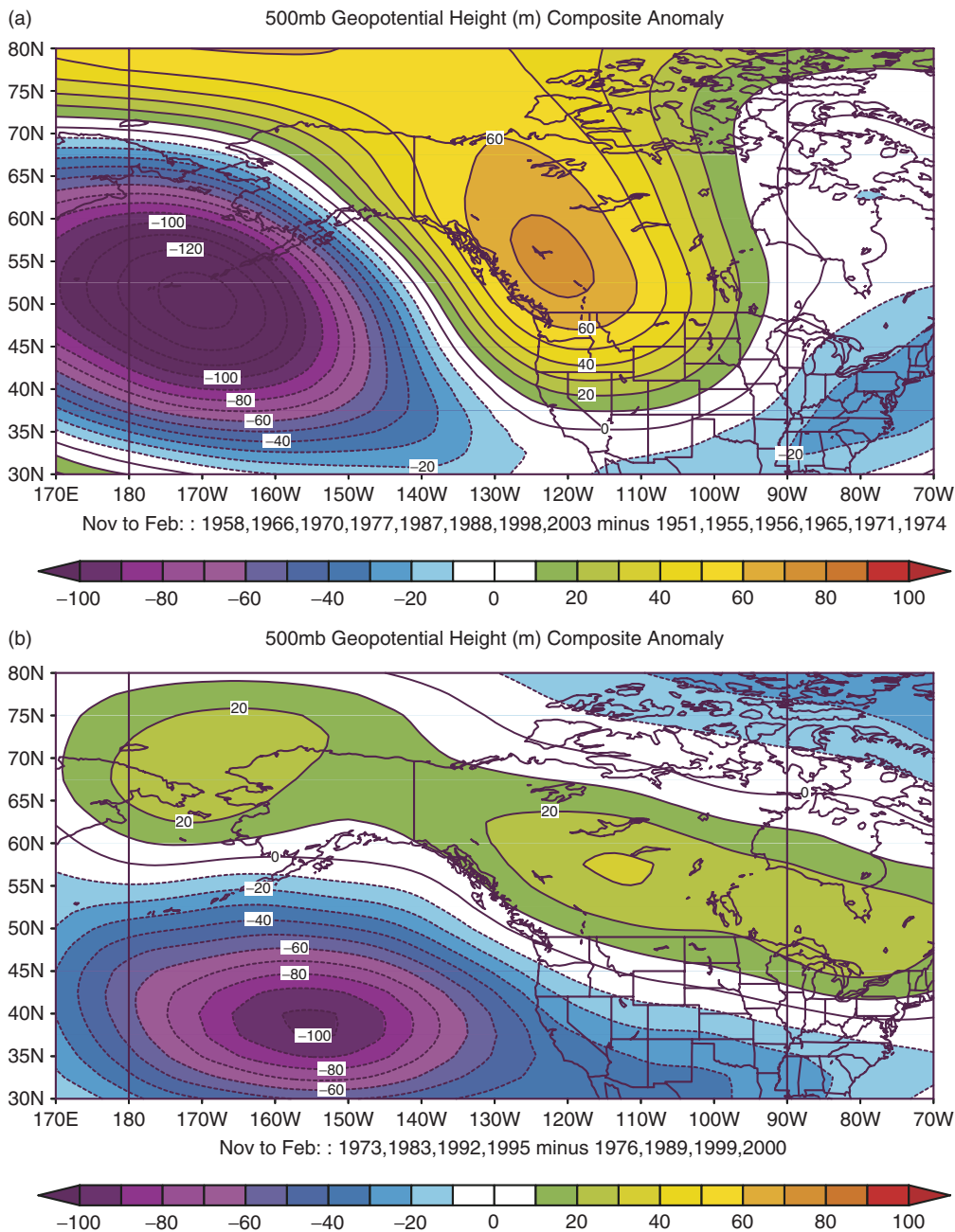
Figure 2. (a) Difference in the mean 500 hPa geopotential height (contour interval 10 m) during the El Niño/AO− winters (1957–1958, 1965–1966, 1969–1970, 1976–1977, 1986–1987, 1987–1988, 1997–1998, and 2002–2003) from that during the La Niña/AO− winters (1950–1951, 1954–1955, 1955–1956, 1964–1965, 1970–1971, and 1973–1974). (b) Difference in the mean 500 hPa geopotential height (contour interval 10 m) during the El Niño/AO+ winters (1972–1973, 1982–1983, 1991–1992, and 1994–1995) from that during the La Niña/AO+ winters (1975–1976, 1988–1989, 1998–1999, and 1999–2000)

there was an average difference of 1.6–1.7 in the AO between the AO− and AO+ winters. A map of the regression of AO against the 500 hPa geopotential height (Figure 5) indicates a very small signal (<10 m for an AO value of unity) in the vicinity of the Aleutians, where there was such a profound distinction in the response to ENSO vis-à-vis the AO (Figure 2(a–b)). Moreover, the AO does not project on the
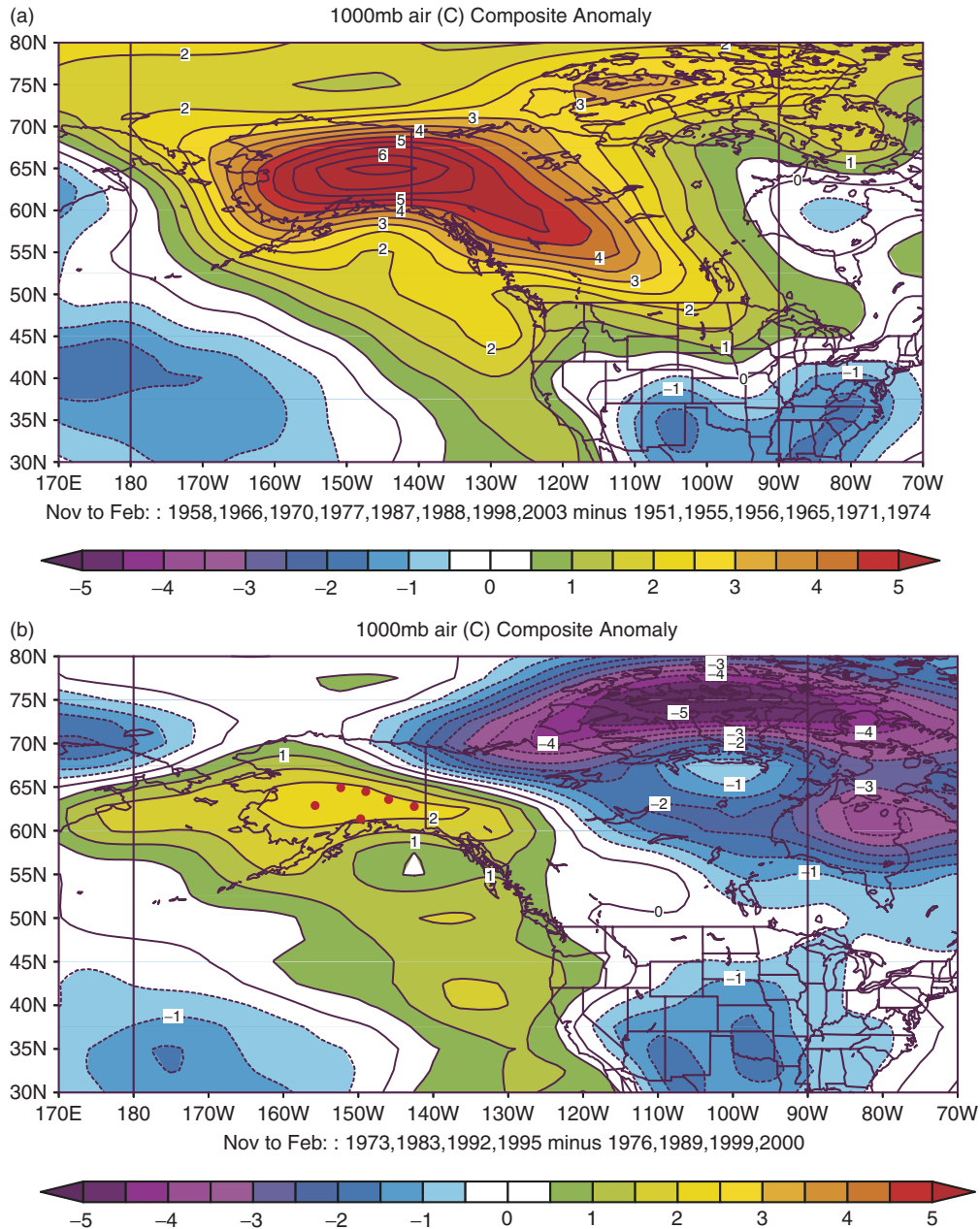
Figure 3. (a) Difference in the mean 1000 hPa temperature (contour interval 0.5 °C) during the El Niño/AO− winters (1957–1958, 1965–1966, 1969–1970, 1976–1977, 1986–1987, 1987–1988, 1997–1998, and 2002–2003) from that during the La Niña/AO− winters (1950–1951, 1954–1955, 1955–1956, 1964–1965, 1970–1971, 1973–1974). (b) Difference in the mean 1000 hPa temperature (contour interval 0.5 °C) during the El Niño/AO+ winters (1972–1973, 1982–1983, 1991–1992, and 1994–1995) from that during the La Niña/AO+ winters (1975–1976, 1988–1989, 1998–1999, and 1999–2000). Red dots indicate the locations of the stations used in surface air temperature computations

meridional component of the flow at 500 hPa over Alaska. The AO is negatively related to the 1000 hPa air temperature in the vicinity of Alaska (Figure 6), but this relationship is strongest for western Alaska and the northern Bering Sea. The discrepancies between the El Niño/La Niña differences in 1000 hPa air temperature (Figure 3(a–b)) are greatest from central Alaska to western Canada. Here the effect of the
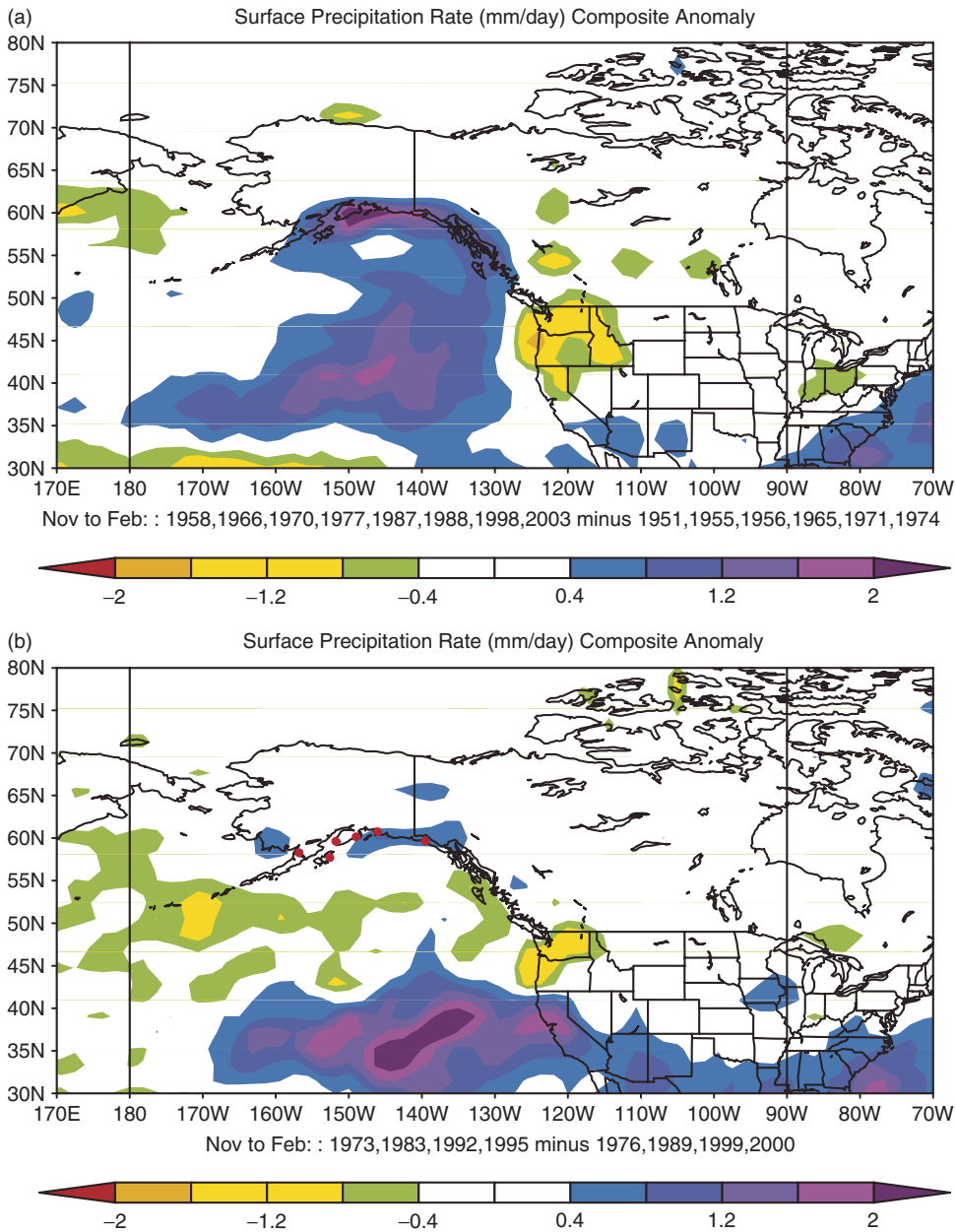
Figure 4. (a) Difference in the precipitation rate (contour interval 0.4 mm day^{-1}) during the El Niño/AO− winters (1957–1958, 1965–1966, 1969–1970, 1976–1977, 1986–1987, 1987–1988, 1997–1998, and 2002–2003) from that during the La Niña/AO− winters (1950–1951, 1954–1955, 1955–1956, 1964–1965, 1970–1971, 1973–1974). (b) Difference in the precipitation rate (contour interval 0.4 mm day^{-1}) during the El Niño/AO+ winters (1972–1973, 1982–1983, 1991–1992, and 1994–1995) from that during the La Niña/AO+ winters (1975–1976, 1988–1989, 1998–1999, and 1999–2000). Red dots indicate the locations of the stations used in precipitation computations

AO by itself (considering the average difference of 1.6–1.7 in the AO) accounts for no more than one-third of the change in the ENSO signal between the AO− and AO+ situations. In summary, the effects of the AO alone fail to explain the character and magnitude of the anomaly patterns shown in Figures 2 and 3.
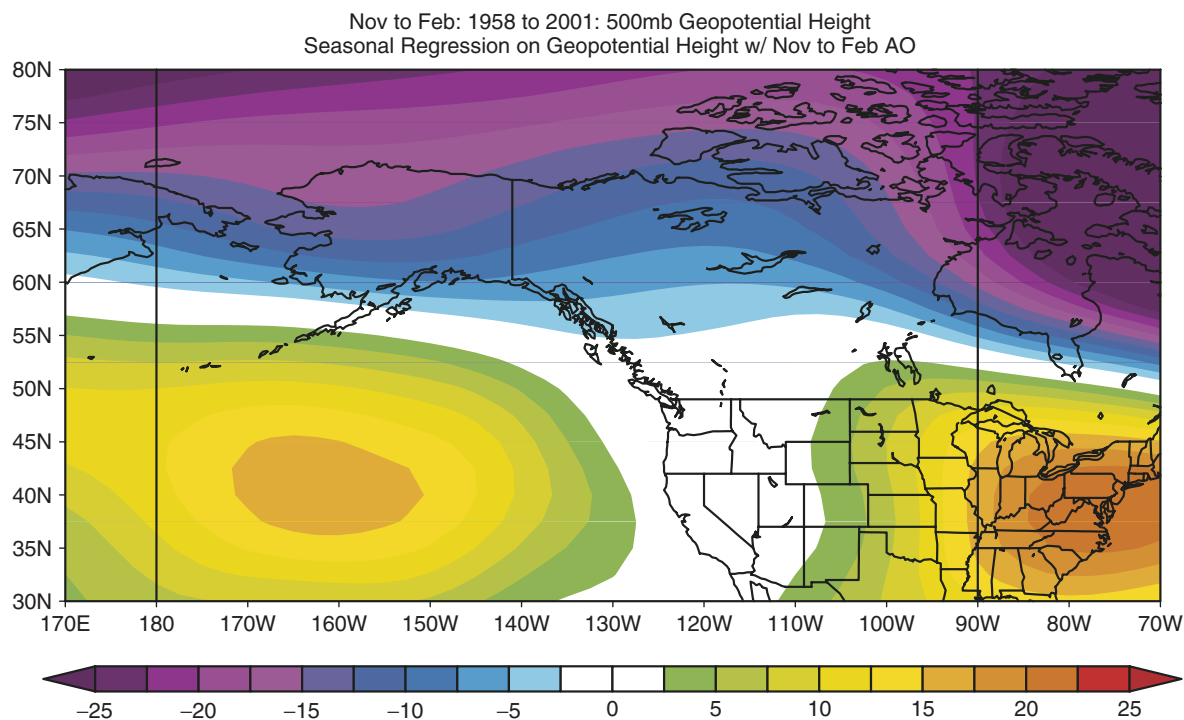
Figure 5. Regression of 500 hPa geopotential height (contour interval 2.5 m) with the AO during winter (November–February) for the period 1958–2001

The ENSO events that constitute the composite results presented above are distributed irregularly over time, and we have examined the extent to which our results can be attributed to long-term trends. The best-fit 55-year linear trends in the seasonal mean 500 hPa geopotential height and the 1000 hPa air temperature were evaluated for the period 1948–2003. This exercise revealed maximum trends of about −1.1 m per year in the 500 hPa height near the negative center in Figure 2(a) and of about 0.06 °C per year in the 1000 hPa air temperature in central Alaska near the positive center in Figure 3(a). Considering that the El Niño/AO− cases occurred on average 19 years after the La Niña/AO− cases, the trends account for roughly 20 m and 1.1 °C of the magnitudes of the extrema in the 500 hPa height and 1000 hPa temperature differences, respectively. Similarly, the El Niño/AO+ cases occurred on average slightly more than five years before the La Niña/AO+ cases, and hence correcting for those trends would imply somewhat stronger ENSO influences than those shown in Figures 2(b) and 3(b). Overall, the trends are responsible for less than 30% of the differences shown in Figures 2 and 3 between AO− and AO+ situations.

The degree to which the composites are typical of the individual events that comprise them is an important issue, especially in situations such as the present, for which relatively few individual realizations are available. We address this issue in the following section.

4. VARIABILITY AMONG CASES

Having about two dozen cases, we have inspected each case individually. Maps of the 500 hPa geopotential height anomaly for each of the events are included in the Appendix; here we present some compact perspectives on the consistency of the results. The composite results indicate strong contrasts in the ENSO signal in terms of the 500 hPa heights in the region of the Aleutian Islands (50 °N, 165 °W). Because of the importance of anomalies found here to the meridional flow into the Bering Sea and Alaska, we first focus
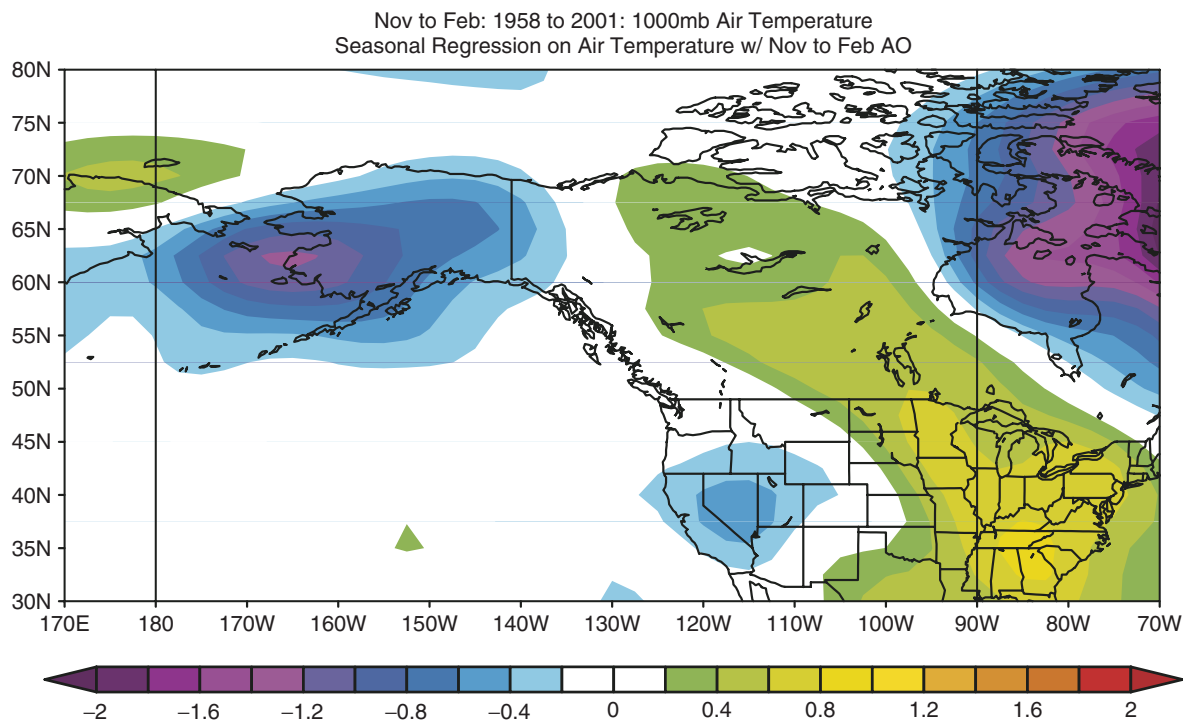
Figure 6. As in Figure 4, but for 1000 hPa air temperature (contour interval 0.2 °C)

on these anomalies in our scrutiny of case-to-case variability. Specifically, the average 500 hPa geopotential height anomaly over a rectangle extending from 45 to 55 °N and 175 to 160 °W for each of the ENSO winters is indicated symbolically in a two-dimensional phase space spanned by the AO and NINO3.4 indices (Figure 7). The pictorial of Figure 7 reprises the composite results shown in the previous section. Even though the mean differences in NINO3.4 are comparable between the pairs of AO− and AO+ winters, there has been a much stronger ENSO effect during AO− conditions. It also shows that this difference is not due to just a few cases dominating the means. For example, six of the eight cases of El Niño/AO− featured strong (>1 standard deviation) negative height anomalies. Only one of these eight cases represents an outlier, the event of 1965–1966, for which there was a strong anomaly of the opposite sign. Similarly, four of the six cases of La Niña/AO− had strong positive height anomalies, with only one case, the event of 1954–1955, having anomalies of negligible magnitude.

Another measure of the mean and variability in the ENSO/AO signal is provided in Table I. Here, for each winter (NDJF) we itemize the mean 500 hPa heights for the region used in Figure 7, and the mean air temperature at six interior Alaska weather stations with long, consistent records. The mean difference in the 500 hPa heights is 123 m between El Niño and La Niña during AO−, with a combined standard error of 36 m, and this difference is 42 m during AO+, with a combined standard error of 40 m. For the interior Alaska air temperature, these two sets of differences are 5.8 °C for AO−, with a standard error of 1.7 °C, and 1.5 °C for AO+, with a standard error of 1.5 °C. It therefore appears that the AO-related contrasts in the mean ENSO signals are sufficiently large, relative to the case-to-case variability, to be statistically robust.

The focus of our analysis has been on the winter season as a whole, but as a means of ascertaining the reliability of the relationship vis-à-vis ENSO and the AO, we have also analyzed monthly data. The value of the AO and of the average 500 hPa geopotential height in the region used for Figure 7 were compiled for each month (NDJF) of the El Niño and La Niña winters. For El Niño, 25 out of a total of 28 months in an AO− state occurred during the winters in which the AO was negative as a whole; 13 out of a total
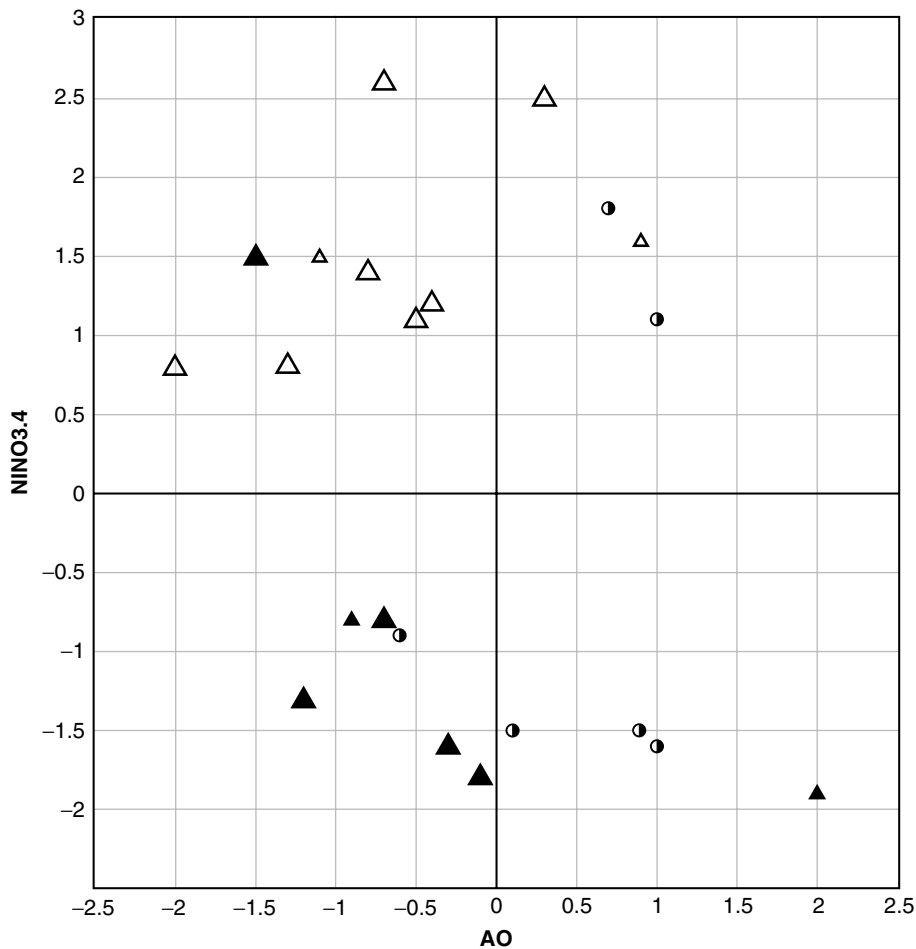
Figure 7. Symbolic representation of the average 500 hPa geopotential height anomaly over a rectangle extending from 45 to 55 °N and 175 to 160 °W for each of the ENSO winters in the phase space spanned by the AO (abscissa) and NINO3.4 (ordinate) indices. Years with small anomalies (<0.25 of the standard deviation in the interannual variability in 500 hPa height) are shown with small, half-filled circles; years with anomalies between 0.25 and 1 standard deviation, and with anomalies greater than 1 standard deviation are shown with small and large triangles, respectively. For the cases with anomalies larger than 0.25 standard deviation, negative anomalies are indicated with solid triangles and positive anomalies are indicated with open triangles. The standard deviation in the height anomaly for the selected rectangle is 58 m

of 20 months in an AO+ state occurred during the winters for which the AO was positive. For La Niña, 20 out of the total of 22 months in an AO− state occurred during AO− winters as a whole, and 14 out of the total of 18 months in an AO+ state occurred during AO+ winters. The 500 hPa heights are 123 m higher on average during El Niño than during La Niña in the AO− months, and this average difference is 52 m for the AO+ months. By way of comparison, their counterparts are 123 and 42 m for the AO− and AO+ winters as a whole.

The larger sample size represented by the monthly data was used in a Student's t test on the significance of the AO's effect on the strength of the ENSO signal. The means and standard deviations (80–100 m) of the monthly values of the 500 hPa heights in each set, and the number of months in each set, yield a t of about 2.5. Given the effective degrees of freedom of ∼21, this value of t implies that the ENSO's effect, in terms of the 500 hPa heights for the prescribed region, is stronger in AO− than in AO+ conditions at the 99% confidence level.

5. THE PACIFIC POLE OF THE AO

While our focus is on the AO's effect on the response to ENSO, our results are pertinent to the controversy related to the Pacific pole of the AO. Regarding this controversy, Deser (2000) emphasizes the lack of coherence between the Pacific and Atlantic poles of the AO, while Wallace and Thompson (2002) argue that a positive correlation between these poles in association with the AO is counteracted by a negative correlation in association with a mode resembling the Pacific-North American (PNA) pattern.

The present study finds that two types of ENSO events, El Niño/AO− and La Niña/AO+, account for a disproportionate fraction of the total signal of the Pacific pole of the AO. To be more specific, we calculated the correlation coefficient between the AO and the 500 hPa geopotential height for a box between 40 to 45 °N and 155 to 165 °W (the Pacific pole of the AO) for the winters (November–February) of 1951–2004. The correlation when including all of the winters was 0.34; excluding the eight El Niño/AO− and four La Niña/AO+ events reduced this correlation coefficient to only 0.15. In other words, these 12 events comprising a bit less than one-quarter of the record account for 80% of the local variance associated with the AO. Our interpretation of this result is that the Pacific pole of the AO is not very robust. Moreover, inspection of the 500 hPa height anomaly maps for the four types of winters indicates more of a PNA-like structure from the southeastern US into the western Atlantic during the El Niño/AO− (Figure 1(a)) and La Niña/AO+ (Figure 1(d)) events than during the El Niño/AO+ (Figure 1(b)) and La Niña/AO− (Figure 1(c)) events.

6. DISCUSSION

The present study extends previous investigations into the average effects of ENSO on Alaska's winter weather by showing that ENSO's impacts are much stronger when the AO is in a negative phase. Under this condition there is a strong tendency for substantial southerly (northerly) flow anomalies aloft during El Niño (La Niña); when the AO is in a positive state the flow anomalies accompanying ENSO are generally weaker and less meridional. This difference in the character of the tropospheric flow is consistent with the response to ENSO in terms of the surface weather. On average, El Niño winters have been 2.5 °C warmer in interior Alaska during AO− than during AO+ conditions; La Niña winters have been 1.8 °C colder in interior Alaska during AO− than during AO+ conditions. The AO− situations have also been accompanied by a much greater ENSO signal in terms of winter precipitation in southern Alaska.

The present study is complementary to that of Quadrelli and Wallace (2002). They examined anomalies associated with the AO (aka NAM) during opposite phases of ENSO. We have shown that the response to ENSO in the vicinity of ENSO depends on the phase of the AO. By aggregating ENSO events according to the sign of the AO, clear distinctions in the mean circulation associated with ENSO are revealed. Our results therefore provide a new perspective on the ENSO signals reported by Papineau (2001).

Our analysis of the interactions between ENSO and the AO pertains to the robustness of the Pacific pole of the AO. We found that ~80% of the variance in the Pacific pole of the AO was associated with two types of winters, El Niño/AO− and La Niña/AO+. In other words, for the last five decades as a whole the AO apparently has had only a minimal manifestation in the North Pacific except when ENSO was substantially anomalous.

The focus of this paper has been on the weather of Alaska, but our results also provide a new perspective on ENSO's effects on Canada and the continental US. The El Niño/La Niña difference map of 500 hPa geopotential height during AO− (Figure 2(a)) indicates a strong ridge of higher heights centered over western Canada extending into the Pacific Northwest and northern Great Plains of the US, while its counterpart during AO+ (Figure 2(b)) indicates a lower-amplitude ridge stretching from Alaska to southeastern Canada. These differences in flow are associated with ENSO signals in 1000 hPa air temperature that include warm anomalies from Alaska across western Canada to the northern Great Lakes and cold anomalies across the southern US during AO− (Figure 3(a)), and only weak warm anomalies in western Canada but strong cold anomalies in north-central to eastern Canada during AO+ (Figure 3(b)). Similarly, the ENSO signal in precipitation includes notable differences vis-à-vis the AO. In particular, the southwestern to south-central portion of the US has not experienced as great an enhancement of rainfall in El Niño *versus* La Niña winters during AO−

conditions (Figure 4(a)) as compared with conditions during AO+ (Figure 4(b)). These discrepancies between different states of the AO help account for some of the inconsistencies in the overall impacts of ENSO on the winter weather of the northern US, as shown by Harrison and Larkin (1998b) and Rodionov and Assel (2003). Our results also extend the findings of Bonsal *et al*. (2001) regarding the interactions of teleconnection modes in terms of Canadian winter temperatures. In particular, while the AO (Bonsal *et al*. considered the closely related North Atlantic Oscillation index) may not have much of an influence on western Canada in the mean, ENSO's effects are strongly dependent on the concomitant state of the AO for western Canada as well as for Alaska.

Much of the current skill in seasonal prediction for the US in winter is associated with ENSO, and the average weather for the canonical ENSO event is strongly weighted in NOAA's CPC forecasts (Ed O'Lenic, 2004, personal communication). We hope that the present work contributes toward the continued improvement of predictions for a major portion of the US and Canada. ENSO events can be anticipated quite reliably, with lead times of a few months to as long as a year, using a variety of statistical and dynamical methods.

Forecasts of the winter mean AO would provide an additional skill for seasonal forecasts. In addition to accounting for the effects of ENSO, information on the AO itself would be useful for Alaska. Unlike most high-latitude regions of the Northern Hemisphere, seasonal mean winter temperatures are inversely related to the mean sense of the AO (Figure 6). While the seasonal mean AO cannot yet be predicted with anything like the skill of predicting ENSO, it is possible that useful skills in its forecast would be forthcoming. Here, it is important to distinguish the short-term (daily to weekly) fluctuations in the AO, which are predictable only out to a week or two, from its mean state over a season. With regard to the latter timescale, the monthly record of the AO for the last 50 years indicates some persistence from fall to winter, perhaps especially during ENSO events. For the cases considered here, when the AO was negative in the fall (September–October), the AO during the following winter (November–February) averaged −0.64 for the El Niños, and −0.53 for the La Niñas. When the AO was positive in the fall, during the following winter it averaged −0.18 for the El Niños and +0.24 for the La Niñas. Additional sources of predictability for the AO include the quasi-biennial oscillation (QBO) as reviewed by Baldwin *et al*. (2001), and perhaps the solar cycle (e.g. Kodera, 2003). The important point here is that it may be possible to develop tools for prediction of the AO on seasonal timescales, and that it would have substantial payoffs for seasonal weather outlooks in the Alaskan region and elsewhere.

APPENDIX

INDIVIDUAL WINTER 500 HPA MAPS

The winter mean 500 hPa geopotential height anomalies for each of the ENSO years used in this paper are shown here. These maps are arranged in groups with the El Niño/AO− events shown in Figure A1(a–h), the El Niño/AO+ events in Figure A2(a–d), the La Niña/AO− in Figure A3(a–f), and the La Niña/AO+ events in Figure A4(a–d). There is good consistency between the members of each group, with the notable exception of the El Niño/AO− winter of 1965–1966 (as pointed out earlier). In summary, the patterns of the circulation anomalies in the composites discussed in Section 3 are clearly representative of most of the component years.
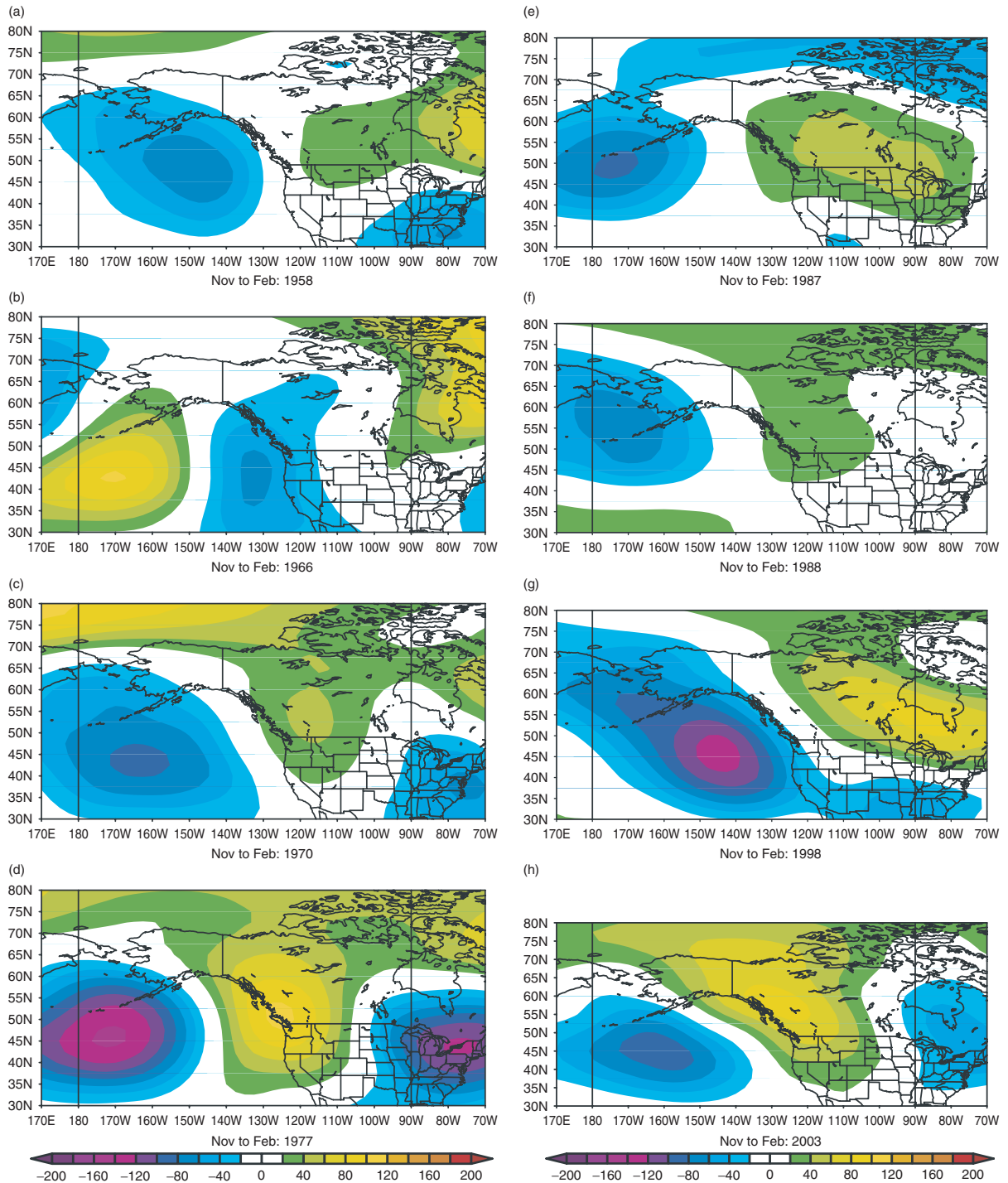
Figure A1. Mean 500 hPa geopotential height anomalies (contour interval 20 m) during November through February for the El Niño/AO− winters of (a) 1957–1958, (b) 1965–1966, (c) 1969–1970, (d) 1976–1977, (e) 1986–1987, (f) 1987–1988, (g) 1997–1998 and (h) 2002–2003. Anomalies are relative to a baseline period of 1968–1996
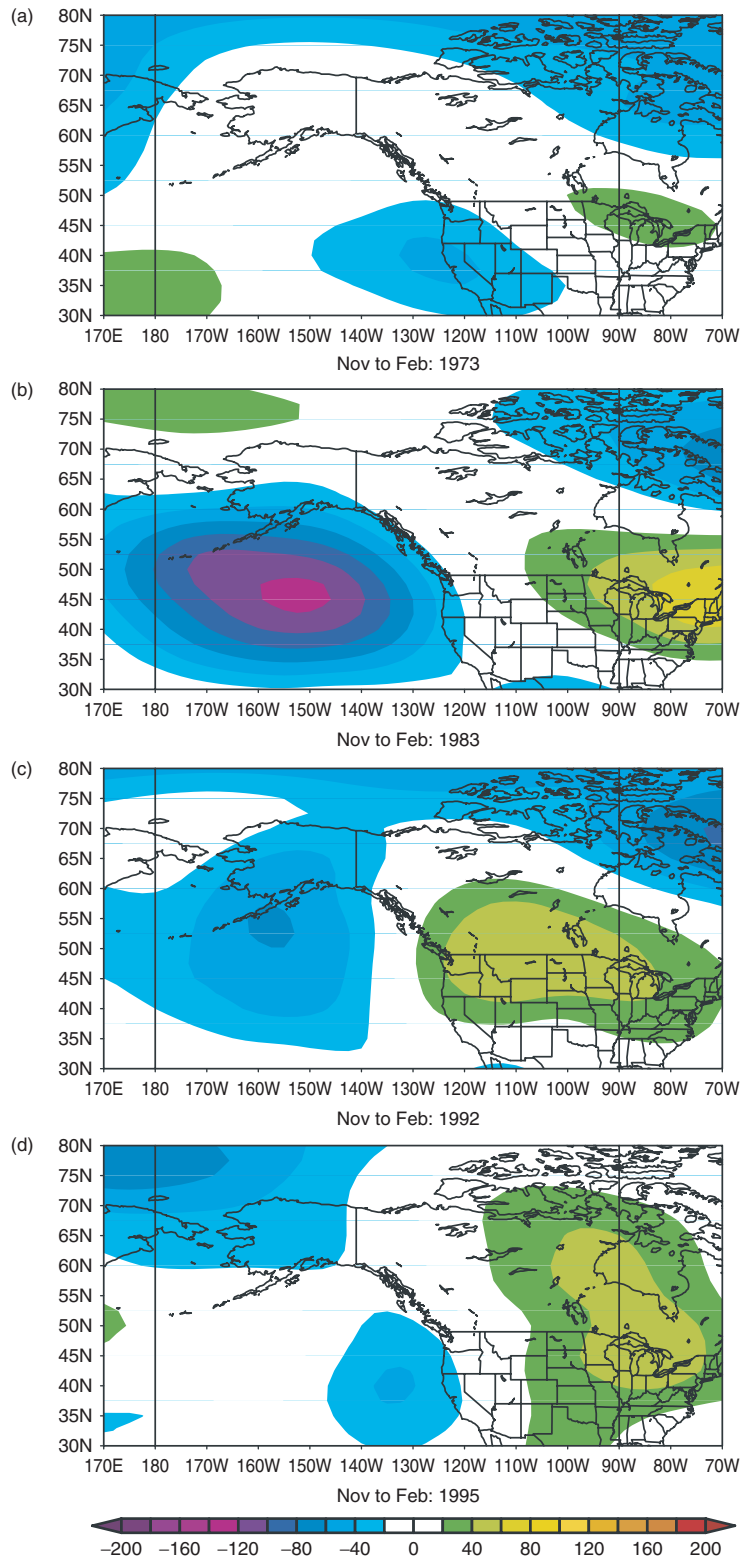
Figure A2. As in Figure A1, but for the El Niño/AO+ winters of (a) 1972–1973, (b) 1982–1983, (c) 1991–1992, and (d) 1994–1995
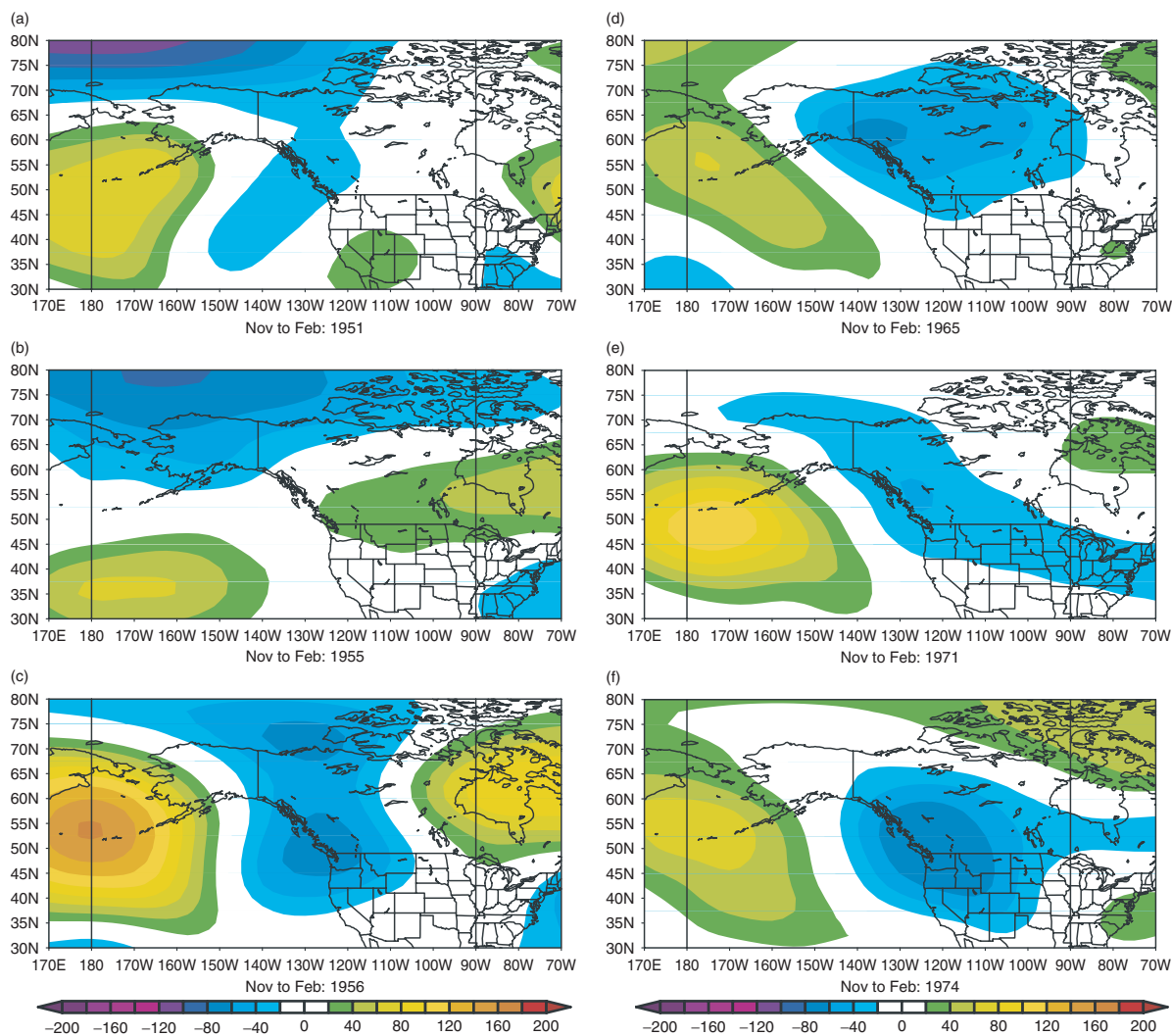
Figure A3. As in Figure A1, but for the La Niña/AO− winters of (a) 1950–1951, (b) 1954–1955, (c) 1955–1956, (d) 1964–1965, (e) 1970–1971, and (f) 1973–1974

OTHER MODES OF NORTH PACIFIC VARIABILITY

ENSO and AO are not the only significant sources of North Pacific atmospheric variability, of course, and the potential influences of other known elements bear some consideration. At the suggestion of a reviewer, we have investigated the relationships between our ENSO/AO results and two other North Pacific patterns of variability, the EAJS (Yang *et al*., 2002) and the WP (a related teleconnection mode), and the PDO (Mantua *et al*., 1997). The objective is to document how the fluctuations in these other indices correspond with the results presented above.

The EAJS represents the quasi-persistent zonal wind jet in the upper troposphere that extends from subtropical East Asia to over the North Pacific. The strength of this jet and the latitude of its core vary, so it is plausible that these variations might have impacts downstream in the area of interest to the present study. The linkage between fluctuations in the EAJS and the results presented above has been evaluated in two ways. First, we compared the phasing between substantial anomalies in the EAJS and the four types of ENSO/AO winters. Following Yang *et al*. (2002), an index for the winter season mean EAJS was computed
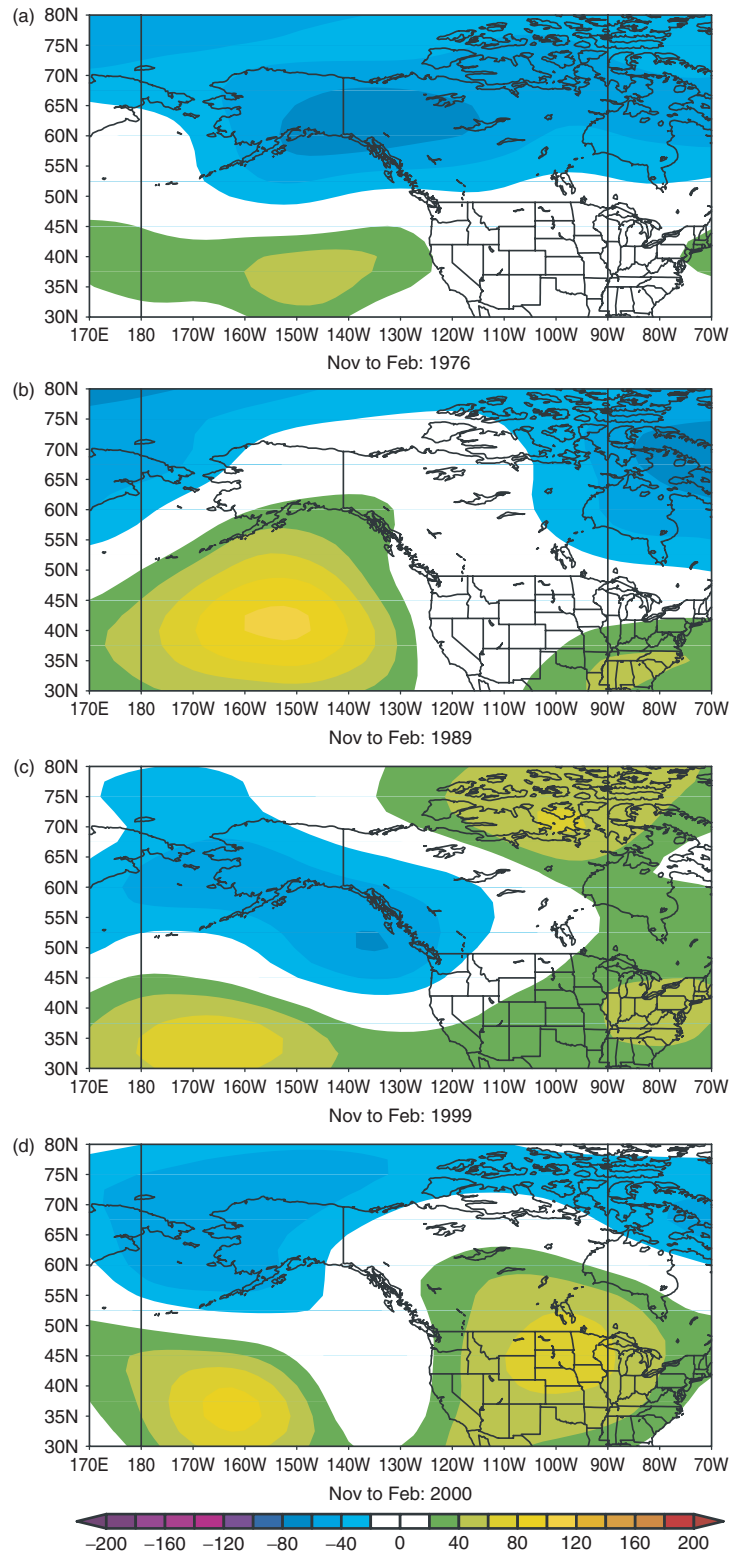
Figure A4. As in Figure A1, but for the La Niña/AO+ winters of (a) 1975–1976, (b) 1988–1989, (c) 1998–1999, and (d) 1999–2000

by averaging the zonal wind at 200 hPa over the region 30–35 °N and 130–160 °E. For the 55-year period of record used in this study, the mean and standard deviation in the 200 hPa zonal wind for this box was calculated; the EAJS is considered strong (weak) during the years when these mean values are more than one standard deviation (3.8 m s^{-1}) larger (smaller) than the mean. This procedure identifies the winters (NDJF) ending in 1962, 1968, 1970, 1977, 1981, 1984, 1985, 1995, 1996, and 2001 as strong EAJS years, and the winters ending in 1954, 1959, 1969, 1972, 1973, 1976, 1979, and 1990 as weak EAJS years. With reference to Table I, this implies that two of the ten strong EAJS years coincided with El Niño/AO− events (1970 and 1977) and one strong EAJS year coincided with an El Niño/AO+ event (1995). Of the eight weak EAJS years, one coincided with an El Niño/AO+ event (1973) and one coincided with a La Niña/AO+ event (1976). These results indicate a minimal correspondence between the years with significant EAJS anomalies and the years in our ENSO/AO sets. The second method by which the influence of EAJS variability was assessed involved simply computing the mean and variability in the EAJS index used above for each set of ENSO/AO winters. This exercise revealed mean values of the EAJS index that are 3.4 m s^{-1} greater during the El Niño than during the La Niña winters in AO− conditions, while the corresponding difference is 0.5 m s^{-1} under AO+ conditions. The standard errors in these differences are ∼2−3 m s^{-1}, which implies that they are marginally distinct from one another in a statistical sense. In summary, it appears that the variability in the EAJS is related to our results based on ENSO and AO to only a moderate extent.

The WP (Wallace and Gutzler, 1981) is another mode of low-frequency variability in the North Pacific. Principally, it reflects fluctuations in the intensity and location of the zonal flow over the western North Pacific. The peak expression of the WP on the zonal winds is about 10–15 degrees north and 30–40 degrees east of the region used for the EAJS index, and time series of the WP and EAJS are only moderately correlated (r ∼ −0.3). Unlike for the EAJS, there is correspondence between our ENSO/AO composites and the state of the WP. During El Niño, the mean value of the WP index is 0.45 and 0.32 for the AO− and AO+ winters, respectively, and during La Niña, its mean value is −0.52 and 0.37 for the AO− and AO+ winters, respectively. The standard errors in these means are 0.2–0.3. The mean values of the WP for the sets of winters indicate that ENSO has an impact on pressure and wind patterns in the western and central North Pacific during AO− conditions, and a negligible effect in AO+ conditions. This result is consistent with the 500 hPa composites shown in Figure 1(a–d). The sense of the implied zonal wind anomalies near 45°N and the dateline is westerly for El Niño/AO− (Figure 1(a)) and easterly for La Niña/AO− (Figure 1(c)), whereas weaker anomalous westerly flow is present during periods of both El Niño/AO+ (Figure 1(b)) and La Niña/AO+ (Figure 1(d)). The nature of the linkage between the WP and the ENSO/AO composite results is discussed at the end of this section.

The relationship of PDO variability to our results is ambiguous. The PDO is based formally on SST anomalies; it has been used to characterize both the state of the upper North Pacific Ocean on short (monthly to seasonal) timescales, and the fluctuations in the North Pacific atmosphere–ocean climate system on decadal timescales. In the latter framework, the PDO has been regarded as a modulating influence on ENSO's effects on air temperatures in Alaska (Papineau, 2001) and Canada (Bonsal et al., 2001). While the PDO certainly represents a signature of the decadal variability in North Pacific climate, it is unclear whether the SST anomalies themselves are an important source of variability. As mentioned in the Introduction, Newman et al. (2003) argue that the PDO reflects largely a response, rather than a cause, of the atmospheric variability that has accompanied the PDO (which itself can be attributed in large part to ENSO). If this is indeed the case, PDO is of little relevance to the present study. Because the nature of the coupling between PDO and North Pacific atmospheric variability remains unsettled, summary statistics for the PDO have been compiled for the years used in our ENSO/AO composites.

These results are itemized in Table AI, which includes both the decadal and seasonal perspectives on the PDO for each set of ENSO/AO winters. As a means of ascertaining the potential influence of the PDO on decadal timescales, counts of the number of events in each set are shown for the overall negative PDO period prior to 1977, the overall positive PDO period of 1977–1998, and the quasi-neutral or 'mixed' PDO period since 1998. The second type of data involves shorter-term information on the state of the PDO. In this regard, Table AI presents mean values of the PDO for the winters in each set, and for the winters preceding those in each set. The latter are included as a measure of the antecedent state of the PDO for each type

Table AI. The PDO during ENSO/AO winters

Type of Winter	<1977	1977–1998	>1998	PDO (−1)	PDO (0)
El Niño/AO−	3	4	1	−0.4	0.9
El Niño/AO+	1	3	0	−0.2	−0.1
La Niña/AO−	6	0	0	−0.5	−1.5
La Niña/AO+	1	1	2	0.4	−1.1

Columns 1–3 refer to the number of events in each category in the predominantly negative PDO period prior to 1976–1977, the predominantly positive PDO period of 1976–1977 to 1997–1998, and the near-neutral or mixed PDO period after 1997–1998. The mean values of the PDO during the winters (NDJF) prior to those in the composites are indicated in column 4; mean values of the PDO for the winters in the composites are indicated in column 5. The values of the PDO index are from http://www.jisao.washington.edu/pdo/.

of ENSO/AO winter. Table AI indicates differences in the state of the PDO for the sets of winters in our ENSO/AO composites, with notable inconsistencies between the results based on the decadal *versus* year-to-year variations in the PDO. For example, while the period of 1977–1998 (when the PDO tended to be positive) included a lower proportion of El Niño/AO− than El Niño/AO+ events, the mean value of the PDO during the former-type winters was substantially greater than that during the latter-type winters. In addition, while all six of the La Niña/AO− events occurred during the period prior to 1977 in which the PDO tended to be negative, and three out of four of the La Niña/AO+ events occurred subsequent to that major shift in the PDO, the mean values of the PDO index during the La Niña/AO− winters are only marginally more negative. Note that there is better consistency between the decadal-scale variations in the PDO and the mean values of the PDO for the four sets of composites when considering the winters preceding the actual ENSO events. It also bears noting that the mean change in the PDO from the preceding winter was markedly positive for the El Niño/AO− events, near-zero for the El Niño/AO+ events, and markedly negative for the La Niña/AO− and La Niña/AO+ events.

The results presented here illustrate the statistical linkages between variations in the WP and PDO indices and the anomalous atmospheric circulations characterizing our ENSO/AO composites. It has been established previously that variations in the PDO are concurrent with those in the strength of the Aleutian low (Mantua *et al.*, 1997, among others). Similarly, considering its loading pattern, the state of the WP relates to the position and strength of the Aleutian low. More prominent geopotential height anomalies are manifested in the vicinity of the mean Aleutian low (near 50°N and the dateline) in association with ENSO during AO− *versus* AO+ conditions, and hence there should exist substantial and systematic differences in the PDO and WP between the sets of winters in our composites. We feel that the simplest explanation of this linkage involves primarily the anomalous atmospheric circulation associated with ENSO and the AO forcing the PDO and WP, but recognize that the nature of our analysis precludes any definitive statements about cause and effect.

It bears noting that both the WP and PDO are significantly correlated with ENSO; the correlation coefficient for each with NINO3.4 is ∼0.45. On the other hand, the correlation coefficient between the AO and NINO3.4 indices for the winter season is only −0.12. The temporal independence of the variations in ENSO and the AO implies that these two indices represent a more complete means of characterizing the lower-order and mostly external influences on the North Pacific atmospheric circulation.

REFERENCES

Baldwin MP, Gray LJ, Dunkerton TJ, Hamilton K, Haynes PH, Randel WJ, Holton JR, Alexander MJ, Hirota I, Horinouchi T, Jones DBA, Kinnersley JS, Marquardt C, Sato K, Takahashi M. 2001. The quasi-biennial oscillation. *Reviews of Geophysics* **39**: 179–229.

Bonsal BR, Shabbar A, Higuchi K. 2001. Impacts of low frequency variability modes on Canadian winter temperature. *International Journal of Climatology* **21**: 95–108.

Deser C. 2000. On the teleconnectivity of the "Arctic Oscillation". *Geophysical Research Letters* **27**: 779–782.

Dole RM, Gordon ND. 1983. Persistent anomalies of the extratropical northern hemisphere circulation: Geographical distribution and regional persistence characteristics. *Monthly Weather Review* **111**: 1567–1586.

Harrison DE, Larkin NK. 1998a. El Niño-Southern oscillation sea surface temperature and wind anomalies. *Reviews of Geophysics* **36**: 353–399.

Harrison DE, Larkin NK. 1998b. Seasonal U.S. temperature and precipitation anomalies associated with El Niño: Historical results and comparison with 1997–1998. *Geophysical Research Letters* **25**: 3959–3962.

Higgins RW, Leetmaa A, Kousky VE. 2002. Relationships between climate variability and winter temperature extremes in the United States. *Journal of Climate* **15**: 1555–1572.

Horel JD, Wallace JM. 1981. Planetary scale atmospheric phenomena associated with the Southern oscillation. *Monthly Weather Review* **109**: 813–829.

Kistler R, Kalnay E, Collins W, Saha S, White G, Woolen J, Chelliah M, Ebisuzaki W, Kanamitsu M, Kousky V, van den Dool H, Jenne R, Fiorino M. 2001. The NCEP-NCAR reanalysis: Monthly means CD-ROM and documentation. *Bulletin of the American Meteorological Society* **82**: 247–267.

Kodera K. 2003. Solar influence on the spatial structure of the NAO during the winter 1900–1999. *Geophysical Research Letters* **30**: 1175, DOI:10.1029/2002GL016584.

Larkin NS, Harrison DE. 2001. Tropical Pacific ENSO cold events, 1946–95: SST, SLP, and surface wind composite anomalies. *Journal of Climate* **14**: 3904–3931.

Mantua NJ, Hare SR, Zhang Y, Wallace JM, Francis RC. 1997. A Pacific interdecadal climate oscillation with impacts on salmon production. *Bulletin of the American Meteorological Society* **78**: 1069–1079.

Newman M, Compo GP, Alexander MA. 2003. ENSO-forced variability of the Pacific decadal oscillation. *Journal of Climate* **16**: 3853–3857.

Niebauer HJ, Bond NA, Yakunin LP, Plotnikov VV. 1999. An update on the climatology and ice of the Bering Sea. In *Dynamics of the Bering Sea*, Loughlin TR, Ohtani K (eds). North Pacific Marine Science Organization (PICES), University of Alaska Sea Grant. Fairbanks, Alaska, USA.

Overland JE, Adams JM, Bond NA. 1999. Decadal variability of the Aleutian low and its relation to high-latitude circulation. *Journal of Climate* **12**: 1542–1548.

Papineau JM. 2001. Wintertime temperature anomalies in Alaska correlated with ENSO and PDO. *International Journal of Climatology* **21**: 1577–1592.

Quadrelli R, Wallace JM. 2002. Dependence of the structure of the Northern Hemisphere annular mode on the polarity of ENSO. *Geophysical Research Letters* **29**: 2132–2135.

Rodionov S, Assel RA. 2003. Winter severity in the great lakes region: A tale of two oscillations. *Climate Research* **24**: 19–31.

Rodionov SN, Overland JE, Bond NA. 2005. The Aleutian low and winter climatic conditions of the Bering Sea. Part I: Classification. *Journal of Climate* **18**: 160–177.

Rogers JC. 1981. The North Pacific oscillation. *Journal of Climatology* **1**: 39–57.

Smith CA, Sardeshmukh P. 2000. The effect of ENSO on the intraseasonal variance of surface temperature in winter. *International Journal of Climatology* **20**: 1543–1557.

Thompson DWJ, Wallace JM. 1998. The Arctic oscillation signature in the wintertime geopotential height and temperature fields. *Geophysical Research Letters* **25**: 1297–1300.

Thompson DWJ, Wallace JM. 2001. Regional Climate Impacts of the Northern Hemisphere annular mode. *Science* **293**: 85–89.

Thompson DWJ, Baldwin MP, Wallace JM. 2002. Stratospheric connection to Northern Hemisphere wintertime weather: Implications for prediction. *Journal of Climate* **15**: 1421–1428.

Wallace JM, Gutzler DS. 1981. Teleconnections in the geopotential height field during the Northern Hemisphere winter. *Monthly Weather Review* **109**: 784–812.

Wallace JM, Thompson DWJ. 2002. The Pacific center of action of the Northern Hemisphere annular mode: Real or artifact? *Journal of Climate* **15**: 1987–1991.

Yang S, Lau K-M, Kim K-M. 2002. Variations of the east Asian jet stream and Asian-Pacific-American winter climate anomalies. *Journal of Climate* **15**: 306–325.